In-depth characterization of layer 5 output neurons of the primary somatosensory cortex innervating the mouse dorsal spinal cord

[1,2]N. Frezel, [3]J.M. Mateos, [3]E. Platonova, [3]U. Ziegler [1,*]H. Wildner, [1,4,*]H.U. Zeilhofer

[1]Institute of Pharmacology and Toxicology, University of Zurich, Winterthurerstrasse 190, CH-8057 Zürich, Switzerland.
[2]Biologie Cellulaire de la Synapse, Inserm U1024, Institute of Biology, École Normale Supérieure (IBENS), 46 rue d'Ulm, Paris 75005, France.
[3]Center for Microscopy and Image Analysis, University of Zürich, Zürich, Switzerland.
[4]Institute of Pharmaceutical Sciences, Swiss Federal Institute of Technology (ETH) Zürich, Vladimir-Prelog-Weg 1-5/10, CH-8090 Zürich, Switzerland

*corresponding authors: Dr. H.U. Zeilhofer & Dr. H. Wildner, [1]Institute of Pharmacology and Toxicology, University of Zürich, Winterthurerstrasse 190, CH-8057 Zürich, Switzerland.
Phone: +41 44 63 55938
Fax: +41 44 635 59 88
e-mail: zeilhofer@pharma.uzh.ch
hwildner@pharma.uzh.ch

Number of pages: 32

Number of figures: 7

Number of tables: 1

Keywords: CCK, corticospinal tract, sensory system, spinal dorsal horn, viral tracing

Running title: **characterization of S1-CST neurons innervating the spinal cord**

Abstract

Neuronal circuits of the spinal dorsal horn integrate sensory information from the periphery with inhibitory and facilitating input from higher CNS areas. Most previous work focused on descending projections originating from the hindbrain. Less is known about the organisation of inputs descending from the cerebral cortex. Here, we identified cholecystokinin (CCK) positive layer 5 pyramidal neurons of the primary somatosensory cortex (S1-CST neurons) as a major source of descending input to the spinal dorsal horn. We combined intersectional genetics and virus-mediated gene transfer to characterize CCK^+ S1-CST neurons and to define their presynaptic input and postsynaptic target neurons. We found that S1-CST neurons constitute a heterogeneous population that can be subdivided into distinct molecular subgroups. Rabies-based retrograde tracing revealed monosynaptic input from layer 2/3 pyramidal neurons, from parvalbumin (PV) and neuropeptide Y (NPY) positive cortical interneurons, and from thalamic relay neurons in the ventral posterolateral nucleus. WGA-based anterograde tracing identified postsynaptic target neurons in dorsal horn laminae III and IV. About 60% of these neurons were inhibitory and about 60% of all spinal target neurons expressed the transcription factor c-Maf. The heterogeneous nature of both S1-CST neurons and their spinal targets suggest sophisticated roles in the fine-tuning of sensory processing.

Introduction

In addition to the hindbrain, the cerebral cortex is a major source of descending input to the spinal cord (Lemon RN and J Griffiths 2005; Abraira VE et al. 2017; Wang X et al. 2017; Liu Y et al. 2018; Ueno M et al. 2018). Layer 5 pyramidal neurons of several cortical areas project to this site, including neurons residing in the motor and premotor cortices as well as in the somatosensory cortex (S1). In rodents as well as in humans, the axons of the corticospinal neurons travel through the internal capsule in the forebrain to enter the cerebral peduncles at the base of the midbrain. They then pass through the brainstem to form the pyramids, at the base of the medulla. The vast majority of the fibres then decussate at this level to enter the spinal cord. From there, the axons of the rodent corticospinal tract (CST) run in the ventral part of the dorsal funiculus, while in humans the tract is located in the lateral white matter.

Most studies on the function of the CST have focused on fine motor control (Wang X et al. 2017; Ueno M et al. 2018) often in the context of spinal cord injury and spinal cord repair (Bareyre FM et al. 2005; Steward O et al. 2008; Fry EJ et al. 2010; Porrero C et al. 2010; Jin D et al. 2015). These studies have targeted either the whole CST, or CST neurons of the motor cortex. The presence of direct synaptic contacts between CST neurons that descend from S1 and spinal interneurons (Abraira VE et al. 2017; Liu Y et al. 2018; Ueno M et al. 2018) suggests that CST neurons also play an important role in somatosensory processing, beyond sensorimotor integration. This is in line with previous findings that CST neurons from the motor (M1) and S1 cortices contact distinct populations of spinal interneurons (Ueno M et al. 2018).

The functional analysis of specific parts of the CST has been in part limited by the lack of tools to specifically target defined subgroups of CST neurons (e.g., CST neurons that descend from a defined cortex area to a specific spinal cord region). Transgenic mouse lines (Bareyre FM et al. 2005; Porrero C et al. 2010) and virus-mediated gene transfer (Hutson TH et al. 2012; Ueno

M et al. 2018) have been used to label axons and terminals of CST neurons in the spinal cord. These studies showed that the CST axons terminate mainly in the laminae III and IV of the dorsal horn, in accordance with earlier tracing studies (Casale EJ et al. 1988), where they contact dorsal horn interneurons (Abraira VE et al. 2017; Ueno M et al. 2018). However, the Emx1 or Thy1-H fluorescent reporter mice used in these studies label many neurons in addition to CST neurons (Bareyre FM et al. 2005; Porrero C et al. 2010; Willenberg R and O Steward 2015; Zeisel A et al. 2015) and therefore do not allow specific targeting of CST neurons for characterization and functional manipulation. To this end, it would be crucial to restrict transgene expression to the layer 5 pyramidal neurons in an area of the cortex (S1 in this case) that projects to the spinal region of interest such as the dorsal horn of the spinal cord. Recently, a new recombinant adeno-associated virus (rAAV) serotype (rAAV2-retro) (Tervo DG et al. 2016) has been developed with greatly improved retrograde labelling efficiency that allows high fidelity tracing of descending inputs to the spinal cord (Haenraets K et al. 2017; Wang Z et al. 2018).

Here, we developed a combination of viral approaches and transgenic mice to specifically label S1-CST neurons. This approach permitted the expression of fluorescent or effector proteins in S1 cortical neurons that project directly to a predefined region of the spinal cord and allowed us to demonstrate that S1-CST neurons with terminations in the spinal dorsal horn constitute a heterogeneous population of neurons that receive monosynaptic input from forebrain sensory circuits and target dorsal horn interneurons known to be involved in the gating of somatosensory and nociceptive signals.

Methods

Animals

Experiments were performed on 6-12-week-old mice kept at a 12:12 h light/dark cycle. Permissions for experiments have been obtained from the Canton of Zurich (permissions 03/2018, 031/2016, and 063/2016). CCK^{cre} mice (Cck<tm1.1(cre)Zjh>/J, (Taniguchi H et al. 2011)) were purchased from Jackson Laboratory. For further details on the genetically modified mice used in this study, see Table 1.

Immunohistochemistry (IHC)

Mice were transcardially perfused with 4% ice-cold paraformaldehyde (in 0.1M sodium phosphate buffer, pH 7.4). Lumbar spinal cord and brain were immediately dissected and post-fixed for 2 hrs with 4% paraformaldehyde (PFA) on ice. Post-fixed tissue was briefly washed with 0.1M sodium phosphate buffer (pH 7.4) and then incubated in 30% sucrose (in PBS) overnight at 4°C for cryoprotection. Cryoprotected tissue was cut at 25 µm or 40 µm (spinal cord or brain, respectively) on a Hyrax C60 Cryostat (Zeiss, Oberkochen, Germany), mounted on superfrost plus glass slides and then incubated with the respective combinations of primary antibodies in 1% donkey serum in phosphate buffered saline (PBS) over-night at 4°C. After brief washes in PBS, sections were incubated with the respective secondary antibodies for 2 hrs at room temperature and briefly rinsed in PBS, before mounting with coverslips and DAKO fluorescent mounting media (Dako, Carpinteria, CA, USA). Secondary antibodies raised in donkey were purchased from Jackson Immuno Research (West Grove, PA, USA). All antibodies used are listed in the Table 1.

Multiplex in situ hybridization (ISH) and image analysis

Spinal tissue used for ISH was dissected from 6-12-week-old mice, collected in 1.5 ml Eppendorf tubes, and immediately frozen in liquid nitrogen. Tissue was embedded in NEG50

frozen section medium (Richard-Allen Scientific), cut into 16 µm sections, and hybridized using the probes designed for RNAscope Fluorescent Multiplex ISH listed in Table 1.

For IHC and ISH, Z-stacks of fluorescent images were acquired on a Zeiss LSM700 confocal and Zeiss LSM800 Airy Scan microscope (Zeiss, Oberkochen, Germany). Numbers of immunoreactive cells in z-stacks were determined using the ImageJ (NIH, Bethesda, Maryland) Cell Counter plugin (Kurt DeVos, University of Sheffield, Academic Neurology).

Intraspinal and cortical virus injections

Viruses were obtained from the resources indicated in Table 1, and used as previously described (Haenraets K et al. 2017). Virus injections were made in adult (6-8-week-old) mice anesthetized with 2% isoflurane and immobilized on a motorized stereotaxic frame (David Kopf Instruments, Tujunga, CA, USA and Neurostar, Tübingen, Germany). For intraspinal injections, the vertebral column was fixed using a pair of spinal adaptors and lumbar spinal cord at L4 and L5 was exposed. Injections (3 × 300 nL) spaced approximately 1mm apart were made at a rate of 50 nL/min with glass micropipettes (tip diameter 30 - 40 µm) attached to a 10 µL Hamilton syringe. For S1 injections, the head was fixed using head bars, the skull exposed and the following injection coordinates were used: (-1; 1.5; 0.8).

Tissue clearing and light sheet imaging

Mice were anesthetized deeply using pentobarbital and perfused transcardially with 10 mL of artificial cerebrospinal fluid (ACSF containing in mM: 125 NaCl, 2.5 KCl, 1.25 NaH_2PO_4, 25 $NaHCO_3$, 1 $MgCl_2$, 2 $CaCl_2$, 20 glucose equilibrated with 95% O_2, 5% CO_2) at room temperature (RT) followed by 200 mL of RT 4% PFA. The perfusion was performed using gravity perfusion setup. Brains were dissected and incubated in 4% PFA overnight, followed by 48 hours incubation in 4% acrylamide (161–0140; Bio-Rad) and 0.25% VA-044 (017–19362; Novachem) in PBS at 4°C. They were then incubated for 3 hours at 37°C for acrylamide polymerization, washed overnight at 37°C in clearing solution (200 mM SDS (L3371; Sigma-

Aldrich) and 200 mM boric acid (L185094; Sigma-Aldrich), pH 8.5), and electrophoresed in clearing solution using an X-CLARITY Tissue Clearing System (Logos Biosystems) for 8 hours at 1.2 A constant current, temperature <37°C, and 100 rpm pump speed. Similar results were obtained by PACT (passive clarity technique, Yang et al., 2014) where samples were incubated in SDS at 37°C over 2 weeks with exchange of the SDS solution every three days. The samples were washed in PBST for 24 hours and incubated in approximately 88% Histodenz (D2158; Sigma-Aldrich) solution in PBS (refractive index adjusted to 1.457) overnight and mounted for imaging in the same solution. Images were acquired using a mesoscale single-plane illumination microscope (MesoSPIM, Version 4) (Voigt F et al. 2019). Briefly, samples were illuminated with an axially scanned light-sheet using Toptica MLE lasers at 488 nm and 561 nm excitation wavelengths. 3D stacks were generated by translating the sample through the light sheet. In the detection path, fluorescent signals were acquired with an Olympus MVX-10 macroscope with a MVPLAPO 1x objective and a Hamamatsu Orca Flash 4.0 CMOS camera. Image analysis were performed with ImageJ and Imaris.

Experimental design and statistical analysis

Cells counts are reported as mean ± SEM. Numbers of experiments (cells or mice) are provided in the figure legends.

Table 1. Materials and reagents

Materials	Resource	Identifier
Mice (shortname)		
C57BL/6J (wild type)	The Jackson Laboratory	IMSR_JAX:000664
C57BL/6.FVB-Tg(Slc6a5-EGFP)13Uze (GlyT2::eGFP)	IPT (Zurich, Switzerland)	MGI:3835459, (Zeilhofer HU et al. 2005)
Cck<tm1.1(cre)Zjh>/J (CCK^{cre})	Jackson Laboratory	(Taniguchi H et al. 2011)
Viral vectors short name		
rAAV9.CAG.flex.eGFP	Penn Vector Core (Philadelphia, PA, USA)	AV-1-ALL854
rAAV-retro/2-shortCAG-dlox-EGFP	VVF (Zurich, Switzerland)	this publication (vHW22-retro)
rAAV-retro/2-shortCAG-tdTomato	VVF (Zurich, Switzerland)	v131-retro
AAV1.CAG.flex.tdTomato.	Penn Vector Core (Philadelphia, PA, USA)	AllenInstitute854
rAAV-retro/2-hEF1a-DreO	VVF (Zurich, Switzerland)	v127-retro
rAAV-retro/2-hCMV-cre	VVF (Zurich, Switzerland)	v36-retro
rAAV-9/2-hEF1α- D_{on}/C_{on}-eGFP	VVF (Zurich, Switzerland)	this publication (vHW18-9)
rAAV-8/2-hSyn1-roxSTOP-dlox-TVA_2A.RabG	VVF (Zurich, Switzerland)	this publication (vHW7-1)
SAD.RabiesΔG.eGFP (EnvA) (EnvA.RV.dG.eGFP)	Salk Institute (La Jolla, CA, USA)	(Albisetti GW et al. 2017)
rAAV2-EF1α-flex-WGA	IPT (Zurich, Switzerland)	this publication
Antibodies (dilution)		
goat anti-Pax2 (1:400)	R&D Systems (Minneapolis, MN, USA)	AB_10889828
guinea pig anti-Lmx1b (1:10 000)	Dr Carmen Birchmeier	(Muller T et al. 2002)
chicken anti-GFP (1:1000)	Life Technologies (Carlsbad, CA, USA)	AB_2534023
rabbit anti-GFP (1:1000)	Molecular Probes (Eugene, OR, USA)	AB_221570
rabbit anti-NeuN (1:1000)	Abcam (Cambridge, UK)	AB_10711153
goat anti-WGA (1:2000)	VECTOR laboratories (Burlingame, CA, USA)	AS-2024
rabbit anti-WGA (1:2000)	Sigma Aldrich (Saint-Louis, MO, USA)	T4144
rabbit anti-c-Maf (1:1000)	Dr Carmen Birchmeier	#40
guinea pig anti-c-Maf (1:1000)	Dr Carmen Birchmeier	#2223, #1 final bleed
rabbit anti-PKCg (1:1000)	Santa Cruz (Dallas, Texas, USA)	AB_632234
rabbit anti-SOM (1:1000)	Santa Cruz (Dallas, Texas, USA)	sc-13099
mouse anti-PV (1:1000)	Swant (Marly, Switzerland)	235
rabbit anti-NPY (1:1000)	Peninsula Laboratories (San Carlos, CA, USA)	T-4069
goat anti-tdTomato (1:1000)	Sicgen (Cantanhede, Portugal)	AB8181-200
RNAscope multiplex FISH probes		
CCK	ACD	Mm-CCK-C1
GFP	ACD	Mm-GFP-C3
RORα	ACD	Mm-Rora-C2
Crhr1	ACD	Mm-Crhr1-C2
Etv1 (Er81)	ACD	Mm-Etv1-O1-C1

Bcl11b (Ctip2)	ACD	Mm-Bcl11b-C1
Htr2c (5-HTR2c)	ACD	Mm-Htr2c-C1
GABARγ1	ACD	Mm-Gabrg1-C1
Plxnd1	ACD	Mm-Plxnd1
Nr4a2 (Nurr1)	ACD	Mm-Nr4a2-C1

IPT: Institute of Pharmacology and Toxicology, University of Zürich; VVF*:* Viral Vector Facility (ETH, Zurich)

Results

Labelling S1-CST neurons in CCK^{cre} mice

We have previously shown that spinal injection of rAAV vectors optimized for axonal infections into the lumbar spinal dorsal horn leads to the transduction of CST neurons in the primary sensory cortex (S1) via infection of their spinal axon terminals (Haenraets K et al. 2017). As recent work (Zeisel et al. (2015)) indicates that layer 5 pyramidal neurons express CCK (Zeisel A et al. 2015), we repeated our initial experiments in CCK^{cre} mice (i.e. mice carrying a knock-in of cre into the CCK gene locus (Taniguchi H et al. 2011)) and injected a rAAV encoding a cre-dependent eGFP into the spinal cord of these mice. This strategy uncovered a population of layer 5 pyramidal neurons in the primary somatosensory cortex that projects directly to the spinal dorsal horn (Fig. 1A). We also found labelled neurons in a few other brain areas, including the anterior cingulate cortex, the thalamus, and the rostral ventromedial medulla (RVM) (Fig. 1B). In all subsequent experiments, we focused on the characterization of CST neurons in the somatosensory cortex. We first tested whether all CST neurons in S1 express CCK^{cre} or whether the CCK^{cre} neurons are a subset of CST neurons. To this end, we co-injected a cre dependent (rAAV2-retro.flex.eGFP) and a cre independent rAAV (rAAV2-retro.tdTomato) into the lumbar spinal cord of CCK^{cre} mice (Fig. 1C). eGFP would then be expressed in CCK^{cre} positive S1-CST neurons, whereas tdTom would label all virus infected neurons connected to the injection site. We found that about 70% (71.5 ± 3.1%) of the tdTom^{+} S1-CST neurons also expressed eGFP. The proportion eGFP^{+} neurons that expressed tdTomato was very similar (75.5 ± 1.6%, Fig.1D).

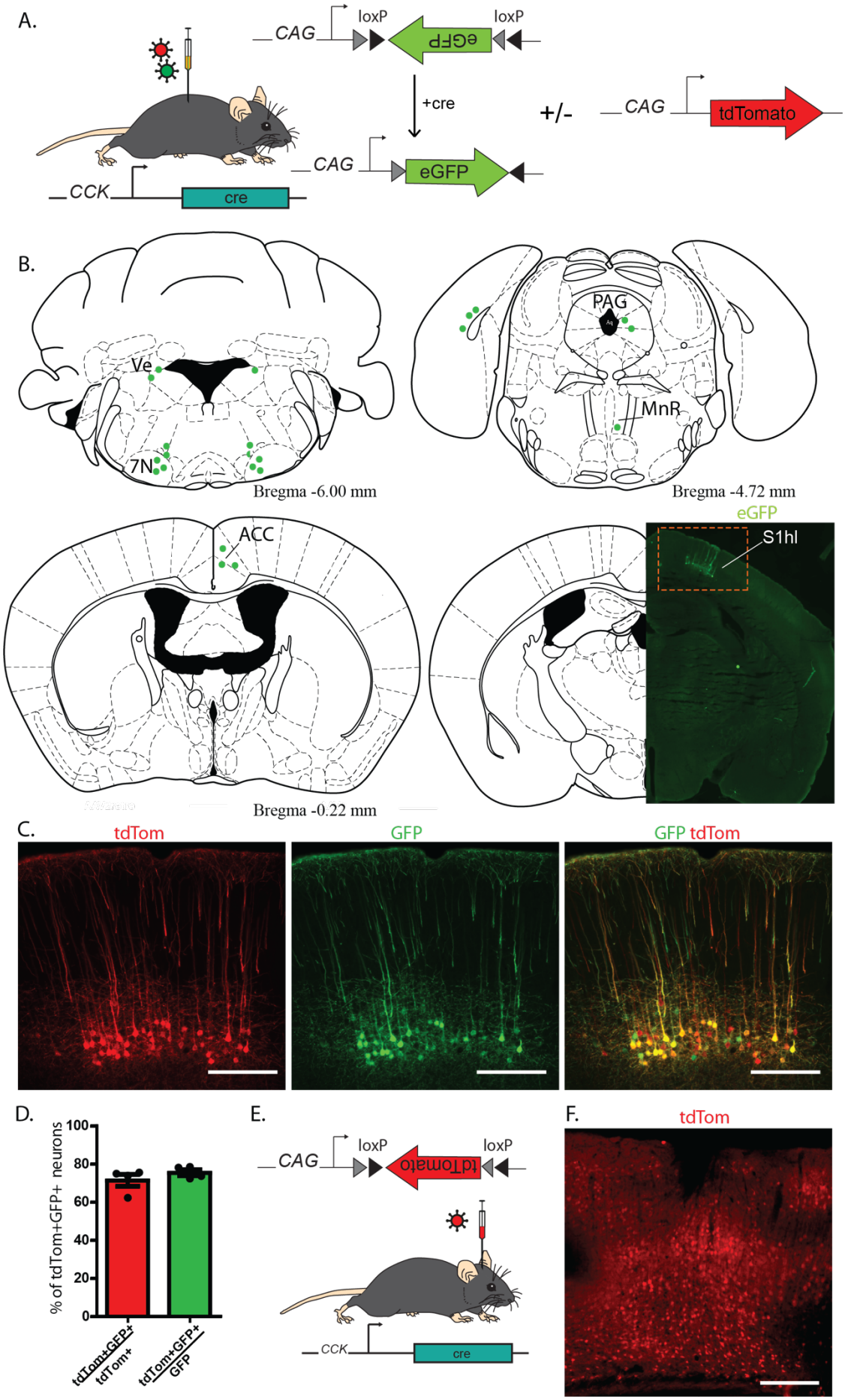
A.
CAG
loxP
eGFP
loxP
+cre
+/-
CAG
tdTomato
CAG
eGFP
CCK
cre
B.
Ve
7N
Bregma -6.00 mm
PAG
MnR
Bregma -4.72 mm
ACC
Bregma -0.22 mm
eGFP
S1hl
C.
tdTom
GFP
GFP tdTom
D.
% of tdTom+GFP+ neurons
100
80
60
40
20
0
tdTom+GEP+
tdTom+
tdTom+GFP+
GFP
E.
CAG
loxP
tdTomato
loxP
CCK
cre
F.
tdTom

Fig.1: Labelling S1-CST neurons in CCK^{cre} mice. (A) Injection of rAAVs encoding for cre-dependent eGFP and cre-independent tdTomato fluorescent proteins into the lumbar spinal cord of CCK^{cre} mice. (B) Brain areas labelled with eGFP positive neurons after intraspinal injection of rAAV9.flex.eGFP in CCK^{cre} mice. 7N: facial nuclei, ACC: anterior cingulate cortex, MnR: median raphe nucleus, PAG: Periaqueductal grey, S1hl: somatosensory cortex, hindlimb area. (C) Comparison of S1-SCT neurons labelled by cre-dependent GFP and cre-independent tdTomato (n = 4, 1546 neurons) fluorescent proteins. (D) Quantification of (C). (E) Injection of rAAVs encoding for cre-dependent tdTomato into the S1 cortex of CCK^{cre} mice. (F) Widespread labelling of cortical neurons with tdTomato (red) after cortical injection (E). Scale bars: 200 µm. Error bars represent ± SEM.

These values are consistent with an expression of CCK^{cre} in the great majority of S1-CST neurons that project to the injection site. S1-CST neurons can hence be efficiently labelled using AAV2retro injections into the dorsal horn of CCK^{cre} mice. However, CCK is not only expressed in cortical layer 5 pyramidal neurons of the mouse cortex but also in a large subset of excitatory and inhibitory neurons of the cerebral cortex (Xu X et al. 2010; Zeisel A et al. 2015). This also became apparent when we injected rAAVs containing a cre-dependent tdTomato directly into the S1 cortex. (Fig.1E-F). As a consequence, injection of rAAVs carrying cre dependent reporter cassettes into CCK^{cre} mice allows anterograde labelling of S1-CST terminals from the cortex and retrograde labelling of their somata from the spinal cord (Fig.2A) but it does not permit a specific transduction of CST neurons only from either of the two injection sites.

Viral targeting strategies to label S1-CST neurons

To overcome this limitation, we developed an intersectional strategy (Fig. 2B) to specifically target CCK^{+} neurons that project from S1 to the spinal cord. To this end, we injected a rAAV2-retro encoding for the Dre recombinase into the lumbar spinal cord of CCK^{cre} mice (Fig. 2B). Subsequently, transduced S1-CST neurons (as well as other CCK^{cre} neurons with processes or somata in the spinal cord) will express both recombinases. Using this strategy, we achieved

targeted expression of the desired transgene by local injection of rAAVs carrying cre- and Dre-dependent transgenes into S1. As a proof of principle, we demonstrate that this strategy works with the injection of a cre- and Dre-dependent rAAV carrying the eGFP transgene (AAV.hEF1α.C_{on}/D_{on}.eGFP) into S1 (Fig. 2B.1). We did not detect eGFP expression outside S1.

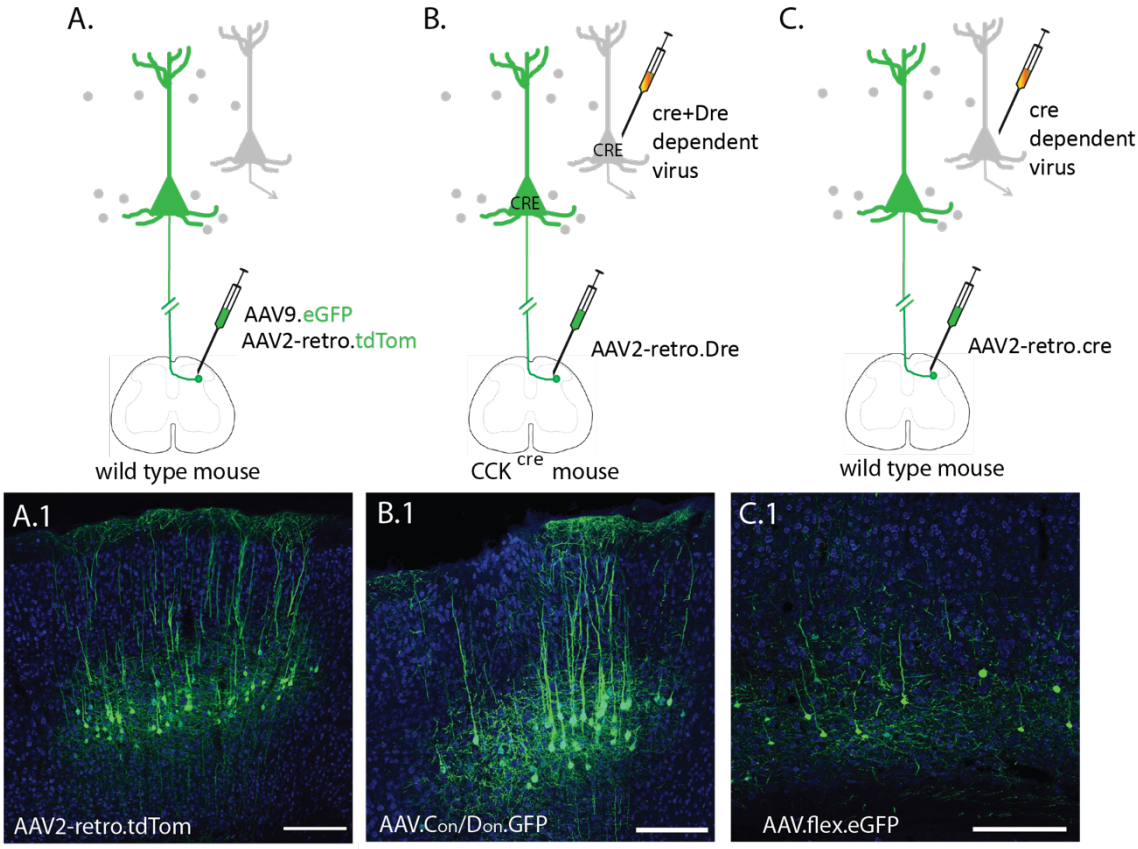

Fig.2: Optimization of the viral targeting strategy to label S1-CST neurons. (A) Retrograde (axonal) transduction of descending neurons from S1 by different recombinant rAAV serotypes. (A.1: example of S1-CST neurons labelling using the rAAV2-retro serotype). (B) Intersectional strategy #1: a rAAV2-retro.Dre is injected into the lumbar spinal cord of a CCK^{cre} mouse, followed by a cortical (S1) injection of a cre-and Dre-dependent rAAV (B.1: example with cortical injection of AVV carrying a transgene for GFP). (C) Intersectional strategy #2: a rAAV2-retro.cre is injected into the lumbar spinal cord of a wild type (WT) mouse, followed by a cortical (S1) injection of a cre-dependent rAAV (C.1: example with cortical injection of rAAV carrying a transgene for GFP). Scale bars: 200 µm.

A possible variation of this intersectional strategy is the injection of a rAAV2-retro.cre into the spinal cord of wild-type mice, followed by the local injection of a rAAV carrying a cre-dependent transgene into S1 (Fig. 2C). This strategy provided even higher labelling efficacy than the first intersectional strategy for eGFP, likely because it required only a single recombination event for transgene expression. As CCK^{cre} positive neurons represent the vast majority of the S1-CST population, the two strategies should label the same neuron population.

Molecular characterization of S1-CST neurons

We next asked whether S1-CST neurons constitute a homogeneous population or are assembled from different subpopulations. To this end, we injected cre dependent rAAV2-retro.flex.eGFP into the spinal cord of CCK^{cre} mice and performed multiplex *in situ* hybridization against several established markers for cortical neurons in cortex sections obtained from the virus-injected mice. We found that all eGFP-labelled neurons expressed the CCK mRNA, demonstrating eutopic expression of the cre transgene in CCK^{cre} mice. Furthermore, the vast majority of eGFP labelled CST-neurons expressed well-established marker genes of cortical layer 5 neurons (Arlotta P et al. 2005; Molyneaux BJ et al. 2007; Watakabe A et al. 2007; Klingler E et al. 2019) including Crhr1 (78.9 ± 4.9%), Er81 (79.2 ± 6.5%), or Ctip2 (80.8 ±2.5%) (Fig.3A, 3B, 3C, respectively). We also found that 48.2 ± 4.0% of $eGFP^{+}$ neurons expressed RORα and 23.5 ± 1.4% expressed Nurr1 (Fig.3D) mRNAs, indicating molecular heterogeneity within the CCK^{+} CST neurons. Expression of several other genes was detected only at low levels in a few $eGFP^{+}$ neurons (gabrg1: 12.8 ± 2.3 %, 5HT2c: 10.37 ± 3.6 %, and Plxnd1: 4.33 ± 1.4 %, Fig.3D and 3E).

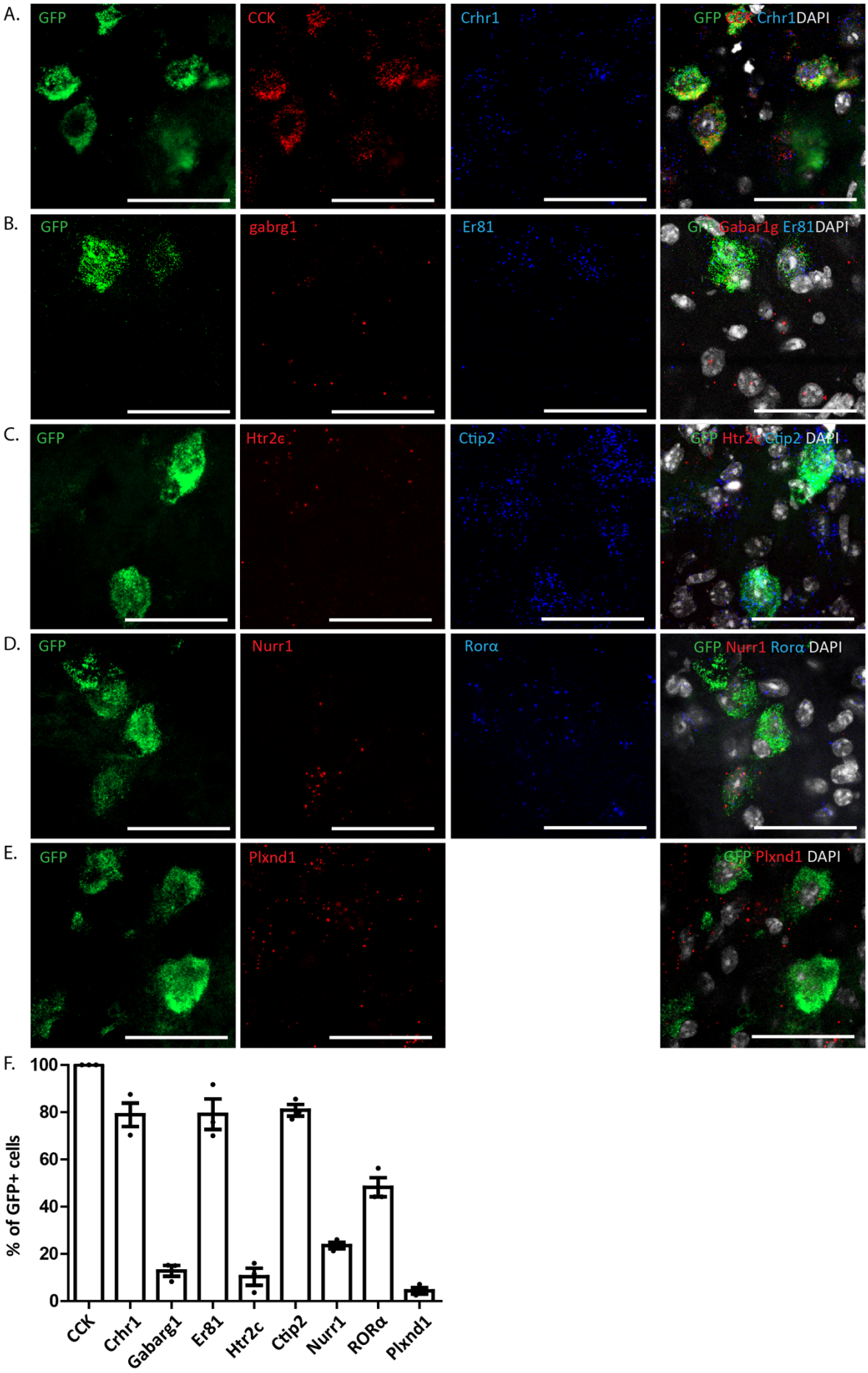
A.
GFP
CCK
Crhr1
GFP CCK Crhr1DAPI
B.
GFP
gabrg1
Er81
GFP Gabar1g Er81DAPI
C.
GFP
Htr2c
Ctip2
GFP Htr2c Ctip2 DAPI
D.
GFP
Nurr1
Rorα
GFP Nurr1 Rorα DAPI
E.
GFP
Plxnd1
GFP Plxnd1 DAPI
F.
% of GFP+ cells
100
80
60
40
20
0
CCK
Crhr1
Gabarg1
Er81
Htr2c
Ctip2
Nurr1
RORα
Plxnd1

Fig.3: Multiplex ISH in GFP-labelled CCK^{cre} neurons with cortical neurons markers in S1. (A-E) Triple ISH showing the colocalization of GFP with CCK and crhr1 (A), htrc2 and ctip2 (B), gabrg1 and er81 (C), nurr1 and rorα (D), Plxnd1 (E). (F). Quantification of (A-E) (n = 3, 352, 221, 85, 243, and 278 GFP neurons respectively). Scale bars: 50 µm. Error bars represent ± SEM.

Morphology of S1-CST neurons

We next examined whether S1-CST neurons send collaterals to CNS regions before they reach the spinal cord. We employed our newly developed strategy to label CCK^{cre} S1-CST neurons as described (Fig.2B). Three weeks after completion of the virus injections, mouse brains were dissected and cleared using the CLARITY procedure. Cleared entire mouse brains were imaged with light-sheet microscopy (Voigt F et al. 2019). The vast majority of S1-CST neuron axons ran from the cortex through the internal capsule and to the midbrain pyramids, following the known trajectory of the CST (Fig. 4) (Wang X et al. 2017). In addition, we detected a few collaterals branching from the main tract at two sites: a small number of axons bifurcated from the internal capsule to terminate in the striatum, and another small group branched-off in the midbrain likely innervating thalamic nuclei (Fig. 4C-E).

Fig.4: Labelling of the corticospinal tract in CLARITY-cleared brain. (A-B) eGFP labelling of S1-CST neurons in a cleared brain. Coronal view (A) and sagittal view (B). White arrow heads indicate collaterals branching of from the main CST towards the dorsal striatum. White arrow indicates collaterals branching of from the main CST towards the ventral thalamus. (C) Higher magnification showing collaterals. Dashed rectangles indicate areas depicted in (D-E). Insets from (C) show axonal projections branching towards the thalamic nuclei (D) and the striatum (E). Scale bars: A: 1000 µm, and B: 1500 µm, C: 150 µm, D: 80 µm, E: 100 µm.

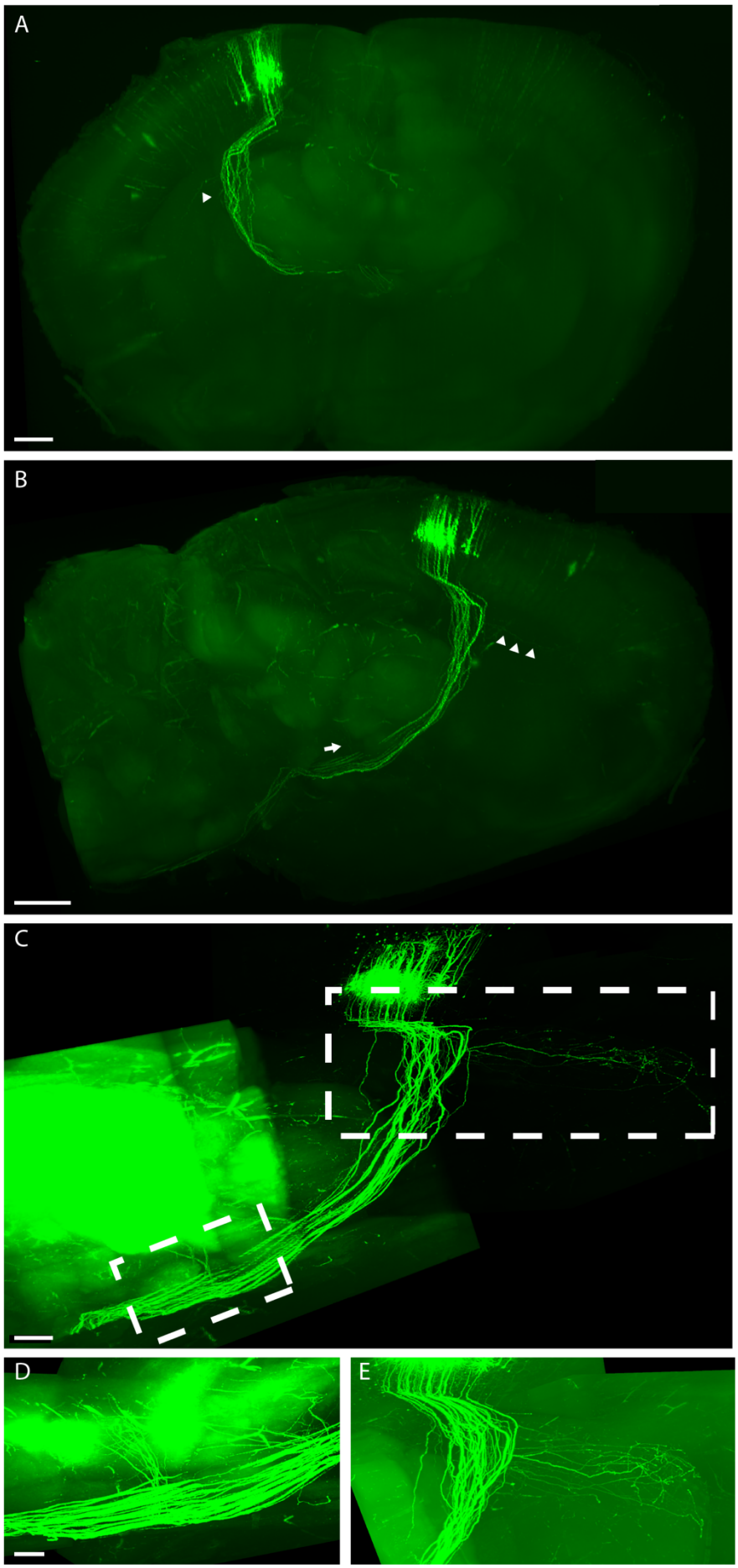
A
B
C
D
E

S1-CST neurons receive input from the somatosensory circuit

The direct connection between the spinal dorsal horn and the somatosensory cortex suggests that S1-CST neurons may be part of a circuit for sensory processing. We sought to further investigate the precise position of S1-CST neurons in this circuit by tracing their presynaptic input and postsynaptic target neurons. We started with the identification of neurons presynaptic to S1-CST neurons and performed monosynaptic retrograde labelling using genetically engineered rabies virus (Callaway EM and L Luo 2015). S1-CST neurons were targeted in CCK^{cre} mice by intraspinal injection of rAAV2-retro.Dre followed by local injection of a cre and Dre dependent helper virus (rAAV.flex.rox.TVA.SAD19-G) into the primary somatosensory cortex S1 (Fig. 5A). The helper virus provided the TVA gene for selective infection by EnvA-pseudotyped rabies virus and the rabies glycoprotein for trans-complementation enabling retrograde labelling across one synapse. We then injected a glycoprotein-deficient EnvA-pseudotyped rabies virus (EnvA.RV.ΔG.eGFP) into the S1 cortex. We found eGFP expressed in layer 5 pyramidal neurons (including the primarily infected S1-CST neurons, Fig. 5B-C) and in many pyramidal neurons of layer 2/3. In layer 5, the rabies virus also labelled interneurons that expressed parvalbumin (PV), in a few cases NPY and rarely somatostatin (SOM) (Fig. 5E-G), three well-characterized markers of cortical inhibitory interneurons (Xu X et al. 2010). We also found $eGFP^{+}$ neurons in the ventral posterolateral nucleus (VPL) of the thalamus (Fig. 5B-D). The morphology of these cells resembled that of previously described thalamocortical sensory relay neurons (Tlamsa AP and JC Brumberg 2010). This connectivity pattern is hence similar to what has previously been described for other CST neurons (Abraira VE and DD Ginty 2013; Constantinople CM and RM Bruno 2013; McMahon et al. 2013). Our results thus demonstrated that CCK-expressing S1-CST neurons are part of a direct sensory circuit loop between the spinal cord, thalamic nuclei and the somatosensory cortex.

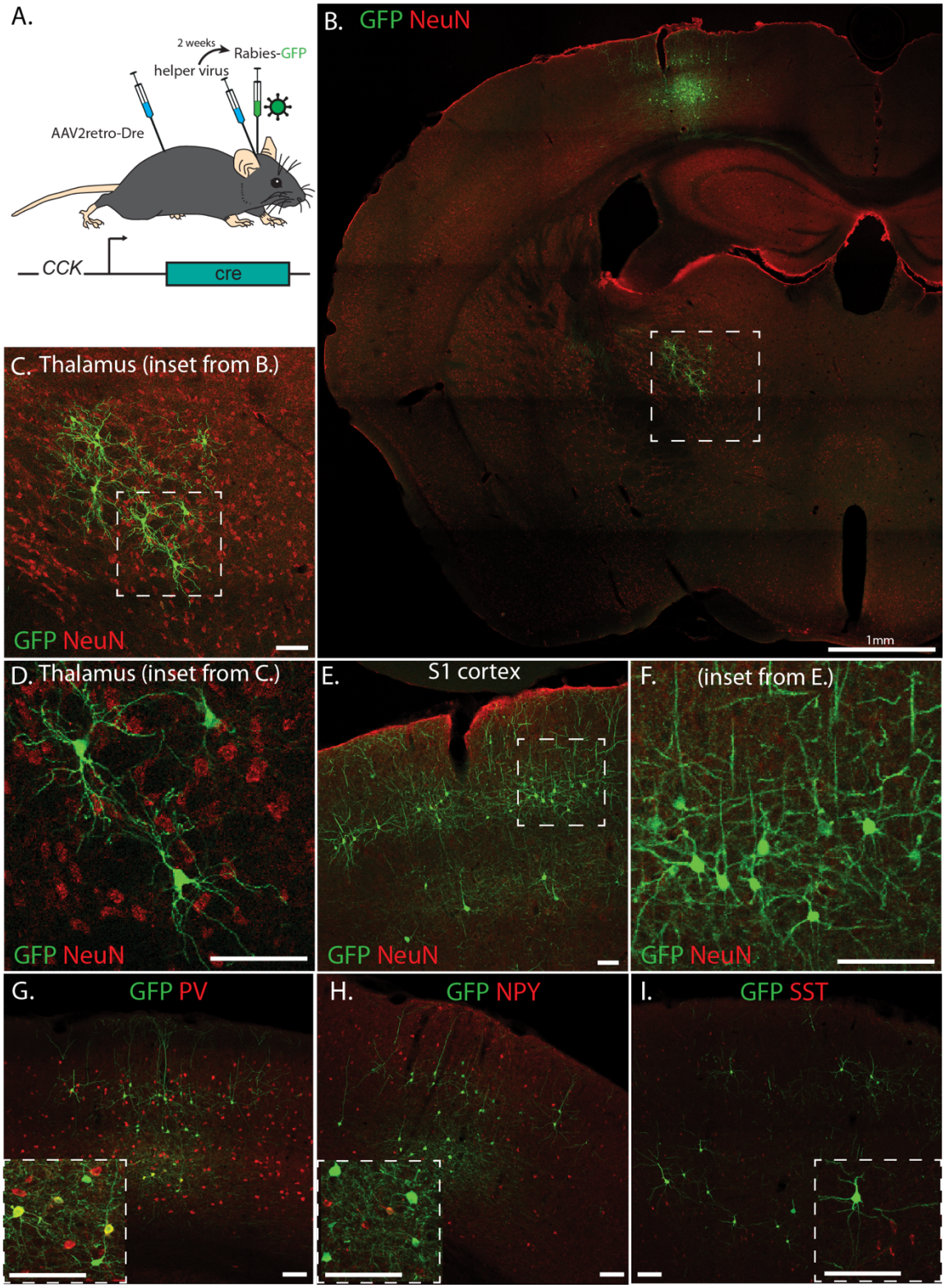

Fig.5: Retrograde monosynaptic tracing of S1-CST neurons with rabies. (A) A rAAV2retro.Dre is injected in the spinal cord of CCK^{cre} mice, followed by a cre-and-Dre-dependent helper virus (TVA, RabG) in S1 and later the pseudotyped rabies virus in S1. (B) Overview of the labelled neurons in the brain: S1-CST neurons

(starter cells) as well as layer 2/3 pyramidal neurons (also in E, F), thalamic sensory relay neurons (C, D), and layer 5 inhibitory interneurons (also in G-I). Scale bars: B: 1 mm; C-I: 100 µm.

Labelling of CST axons in the spinal cord

We next identified the termination area of S1-CST neurons in the lumbar spinal cord (Fig. 6). Injection of rAAV1.flex.tdTomato in the somatosensory cortex hindlimb area (S1hl) of CCK^{cre} mice (Fig. 6A) labelled CST axons in the ventral part of the spinal dorsal funiculus (Fig. 6B, "CST"). Terminals were also visible within the grey matter mainly of the deep dorsal horn (laminae III and IV) (Fig. 6B). This finding is consistent with previous reports of labelling spinal interneurons targeted by CST neurons, showing that tracing from the motor cortex labels terminals mainly in the ventral and intermediate spinal cord, whereas tracing from S1 labels terminals in lamina III and IV of the dorsal horn. (Kamiyama T et al. 2015; Wang X et al. 2017; Ueno M et al. 2018). The dorsal horn laminae III and IV contain interneurons that process touch and proprioceptive information. These laminae also constitute the termination area of low-threshold mechanoreceptive fibres (LTMRs) (Abraira VE et al. 2017). We therefore decided to identify the spinal neurons that are targeted by S1-CST neurons in this region.

Fig.6: **Labelling of the output of S1-CST neurons in the spinal cord. A.** rAAVs carrying either a cre-dependent tdTomato or WGA transgene are injected in S1hl of CCK^{cre} mice. **B.** Labelling of the CST in the dorsal funiculus of the spinal cord, contralateral to the brain injection site. CST terminals are preferentially located below the laminae II-III border marked by PKCγ immunoreactivity. **C-F**. Co-labelling of WGA positive neurons in the spinal cord with the excitatory marker Lmx1β (C**.** and inset) and the inhibitory marker Pax2 (D. and inset). WGA positive neurons also express GFP (E.) and the transcription factor c-Maf (F**.**). G. Quantification of the number of WGA positive neurons that express Lmx1β (n=4, 243 neurons), Pax2 (n = 8, 391 neurons), GlyT2 (n=3, 275 neurons), c-Maf (n=6, 506 neurons) or PKCγ (n = 4, 201 neurons). Error bars represent ± SEM, Scale bars: 100 µm.

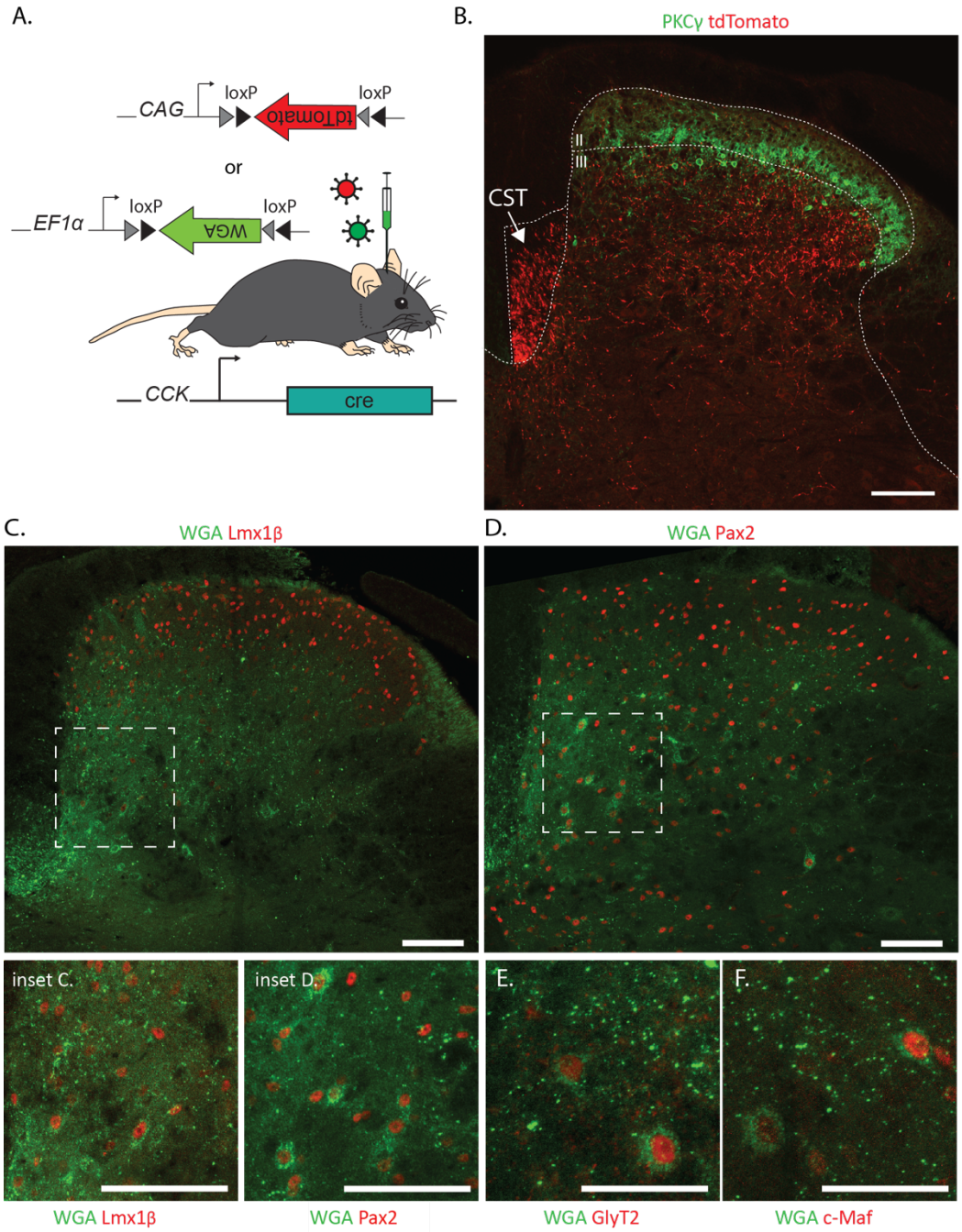
A.
CAG
loxP
tdTomato
loxP
or
EF1α
loxP
WGA
loxP
CCK
cre
B.
PKCγ tdTomato
CST
II
III
C.
WGA Lmx1β
D.
WGA Pax2
inset C.
inset D.
E.
F.
WGA Lmx1β
WGA Pax2
WGA GlyT2
WGA c-Maf

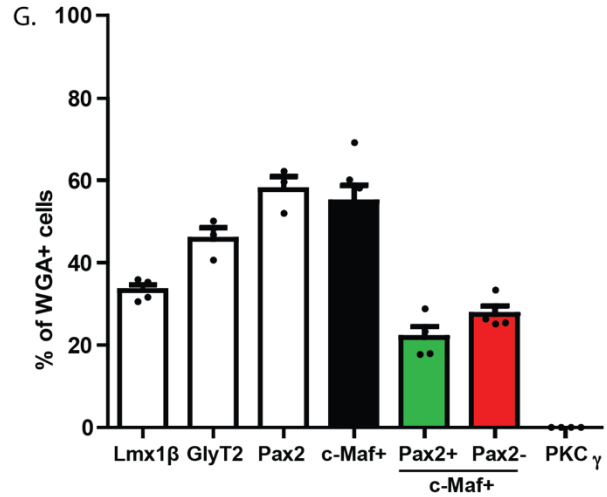
G.
% of WGA+ cells
100
80
60
40
20
0
Lmx1β
GlyT2
Pax2
c-Maf+
Pax2+
Pax2-
PKC γ
c-Maf+

Anterograde transsynaptic tracing with Wheat Germ Agglutinin (WGA)

We used WGA to label neurons that are targeted by S1-CST neurons. CCK^{cre} mice were injected with rAAV2.flex.WGA into S1hl. WGA is transported transsynaptically to label postsynaptic neurons. After 10 days, we detected WGA in the dorsal horn of the lumbar spinal cord (Fig. 6C-G). As expected, WGA immunoreactivity was mostly found in the deep dorsal horn, in lamina III and IV (Fig. 6C-D). In order to identify the neurons that were labelled with WGA, we performed immunocytochemistry against known markers of different dorsal horn interneuron populations. We found that about one third of the WGA labelled neurons were positive for Lmx1β (27.8 ± 1.3%), which is expressed by most excitatory interneurons in laminae I-III express Lmx1β (Del Barrio MG et al. 2013; Albisetti GW et al. 2019) (Fig. 6C, G). More than half of the labelled neurons (56.9 ± 2.1%) were positive for Pax2, a marker of inhibitory neurons of the dorsal horn ((Del Barrio MG *et al.* 2013; Albisetti GW *et al.* 2019) (Fig. 6D, G). When performing anterograde tracing in animals crossed to GlyT2::eGFP mice, a little less than half of all WGA positive dorsal horn neurons (47.8 ± 2.8%) were eGFP+ indicating that they were glycinergic (Jursky F and N Nelson 1995; Poyatos I et al. 1997; Spike RC et al. 1997; Zeilhofer HU *et al.* 2005). Notably, we found that more than half of all WGA positive neurons also expressed the transcription factor c-Maf (54.8 ± 3.9%). Because c-Maf is present in both excitatory and inhibitory dorsal horn interneurons (Hu J et al. 2012; Del Barrio MG *et al.* 2013), we determined the proportion of WGA and c-Maf double-positive neurons that were either inhibitory (Pax2 positive: 21.9 ± 2.6% of all WGA^{+} neurons) or excitatory (Pax2 negative: 27.5 ± 1.9% of all WGA+ neurons). We did not find any WGA positive neuron that was also positive for protein kinase C γ (PKCγ), a marker of a rather small subpopulation of excitatory dorsal horn neurons located at the border between lamina II and III (Malmberg AB et al. 1997; Polgar E et al. 1999). These results suggest that S1-CST neurons

contact a rather heterogeneous population of interneurons in the dorsal horn, including glycinergic neurons and c-Maf expressing neurons.

Discussion

In the present study, we developed intersectional rAAV-based strategies to characterize S1-CST neurons that innervate the spinal cord. We found that these neurons constitute a molecularly heterogeneous group of neurons that in turn innervate a heterogeneous target population in the spinal dorsal horn. Furthermore, we show that they receive direct input from sensory thalamic relay neurons in addition to intracortical synaptic input from layer 2 pyramidal and from NPY and PV positive interneurons. These results establish a long-range feedback loop between the sensory spinal cord and the output neurons of the primary somatosensory cortex (Fig. 7).

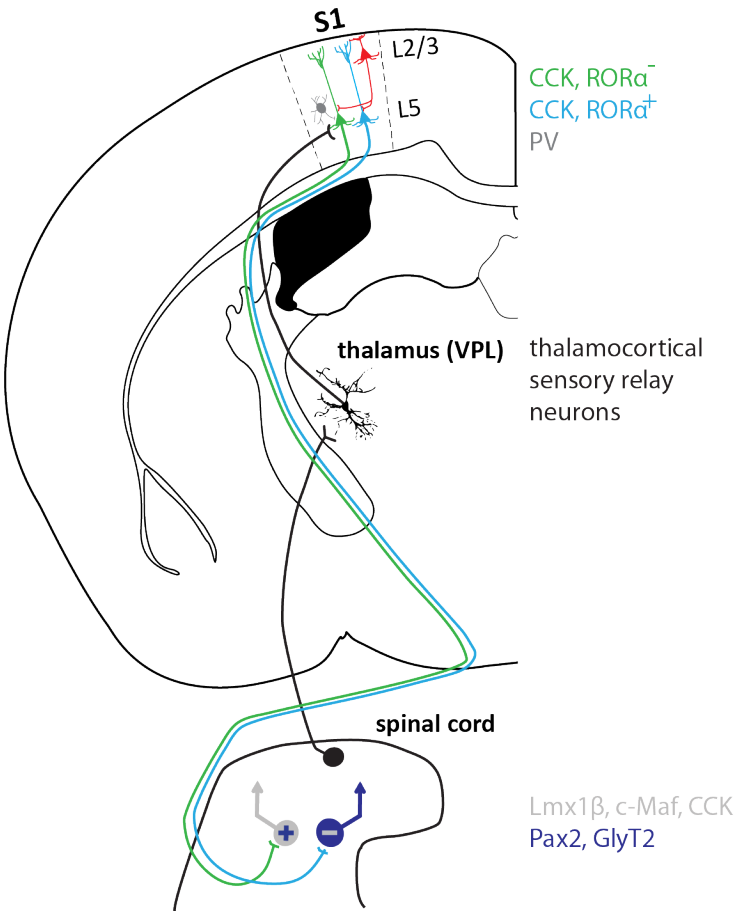

Fig.7: **Model of a spinothalamocortical feedback circuit**

Spinal projection neurons relay sensory information to the ventral posterolateral nucleus wof the thalamus (VPL). Sensory thalamocortical relay neurons propagate the information directly to CST neurons in S1. S1-CST neurons also receive direct synaptic input from inhibitory (PV) neurons and pyramidal layer 2/3 neurons. We postulate that different subpopulations of CST neurons (e.g. RORα^{+} or RORα^{-}) project back onto different types of spinal interneurons (e.g. inhibitory (GlyT2^{+}, Pax2^{+}) or excitatory (Lmx1β^{+}, CCK^{+}, c-Maf^{+}) and thus exert potentially modality specific functions.

S1-CST neurons in somatosensory circuits

In contrast to previous studies, we specifically targeted lumbar spinal cord projecting CST neurons in S1, thus enabling circuit analysis at an unprecedented resolution. Taking advantage of this, we were able to conduct retrograde monosynaptic tracing with rabies virus. Our experiments revealed that S1-CST neurons receive direct intracortical input from layer 2/3 pyramidal neurons as well as from inhibitory PV, and to a lesser extend from NPY and SOM interneurons. In addition, we also identified direct input from sensory relay neurons in the VPL of the thalamus. This nucleus receives input from the postsynaptic dorsal column, the direct dorsal column pathway and the spinocervical tract that are known to propagate tactile information from the periphery to the brain (Abraira VE and DD Ginty 2013). Our data therefore indicates that CST neurons in S1 integrate direct ascending spino-thalamic sensory information with intra cortical input from layer 2 pyramidal and from mostly PV+ inhibitory interneurons.

This is in agreement with the long-held view that sensory information relayed via the thalamus to the cortex is pre-processed by propagation from cortical layer 4 to layer 2/3 neurons, before arriving at the main output neurons of the somatosensory cortex located in the layer 5 (Gilbert CD and TN Wiesel 1979; Harris KD and GM Shepherd 2015). Moreover, it is also in agreement with *in vivo* evidence indicating the existence of direct connections between the thalamus and layer 5 neurons (Constantinople CM and RM Bruno 2013). The authors of the latter study suggested however that intracortical input may not be necessary for sensory evoked activity in

layer 5 neurons. Bridging these opposing views, Quiquempoix et al. (Quiquempoix M et al. 2018) provided evidence that layer 2/3 pyramidal neurons primarily play a major role in tuning/amplifying sensory evoked responses in cortical output neurons of layer 5.

When analysing the output of S1-CST neurons, we found evidence that, although they mainly project through the CST onto the spinal dorsal horn, they also send collateral branches to the dorsal striatum and the midbrain. This confirms and further specifies previous experiments in which CST collaterals were observed when all spinally projecting neurons were labelled (Wang X et al. 2017; Wang Z et al. 2018). Our data therefore indicate that while their main target is the spinal dorsal horn, S1-CST neurons also contribute to cortico-striatal projections and may thereby influence goal-directed behaviours (Wang X et al. 2017).

Molecular heterogeneity and functional implications

The results presented in this study suggest that S1-CST neurons are not a homogenous set of neurons but can be subdivided into subsets of neurons that differ in their molecular signature. The great majority, perhaps even all, CST neurons in S1 express CCK, in addition to other well-established markers of cortical layer 5 neurons such as Ctip2 and ER81 (Arlotta P et al. 2005; Molyneaux BJ et al. 2007). However, other genes such as the nuclear receptors RORα (48.2%) or Nurr1 (23.5%) are only expressed in subsets of CCK^+ CST neurons. RORα and Nurr1 are nuclear receptors capable of driving specific transcriptional programs, suggesting that the subpopulations marked by the expression of the respective genes can be distinguished by a number of molecular markers. It is possible that this molecular heterogeneity translates into a functional heterogeneity of S1-CST neurons, comparable to what has been observed for other populations of cortical output neurons (Klingler E et al. 2019). Consistent with such a functional heterogeneity, our anterograde tracing experiments revealed that CCK^+ S1-CST neurons target different populations of spinal interneurons, with excitatory and inhibitory phenotypes being about equally prevalent among dorsal horn S1-CST target neurons. A large

portion of the inhibitory target neurons were glycinergic neurons and the majority of the excitatory neurons expressed c-Maf. We have previously demonstrated that glycinergic dorsal horn neurons are an integral part of the spinal gate that controls spinal pain and itch relay (Foster E et al. 2015). Conversely, deep dorsal horn excitatory neurons have been linked not only to fine motor control (Bourane S et al. 2015) but also to chronic pain states (Peirs C et al. 2015; Cheng L et al. 2017; Liu Y et al. 2018). The c-Maf+ neurons identified in the present study are likely a subset of dorsal horn CCK^+ excitatory interneurons (Haring M et al. 2018), whose activation is strongly linked to chronic pain states (Liu Y et al. 2018). Although unproven, it is very well possible that excitatory and inhibitory S1-CST target neurons are innervated by distinct subsets of S1-CST neurons. The activation of all CST neurons in optogenetic or chemogenetic experiments would then activate both inhibitory and excitatory spinal interneurons with potentially opposing effects on sensory processing.

Outlook and future directions

Most studies of the CST focus on its input to the ventral horn and on fine motor control (Wang X et al. 2017; Ueno M et al. 2018; Wang Z et al. 2018), or spinal cord injury and repair (Steward O et al. 2008; Fry EJ et al. 2010; Jin D et al. 2015). Although it is known that S1-CST neurons also innervate the dorsal spinal cord, relatively little is known about their role in the modulation of sensory processing. The conditions under which this specific population of CST neurons is active are also mostly unknown. In a recent study, Liu et al. (Liu Y et al. 2018) observed changes in light touch sensitivity after ablation or silencing of S1-CST neurons, and hence proposed a role of S1-CST input on the processing of tactile input in naïve and neuropathic states. This action occurred via excitatory dorsal horn interneurons targeted by S1-CST neurons.

Here we show that a little less than half of the S1-CST target neurons in the spinal cord are excitatory whereas the remaining target neurons are inhibitory. Future studies will therefore

need to clarify whether these functionally different subpopulations of spinal target neurons are innervated by the same or distinct subsets of S1-CST neurons. Taking advantage of the targeting strategies presented here, it will be possible to drive expression of various reporter or effector proteins in molecular distinct subsets of S1-CST neurons (e.g. RORα+ neurons) in order to analyse their circuit integration and address their function. Alternatively, retrograde tracing initiated at the level of a specific spinal target populations may be used in order to identify and functionally interrogate subpopulations of S1-CST neurons. Self-inactivating rabies virus such as those recently developed by Ciabatti et al. (Ciabatti E et al. 2017) may be suitable to functionally manipulate the S1-CST neuron population that innervates the respective spinal target populations. Finally, our study highlights the importance of spatially restricted and intersectional manipulation of either CST or spinal neurons that express a given marker gene, as several of the genes that we and others found expressed in CST neurons are also present in spinal cord neurons (e.g. CCK, RORα or PKCγ).

Acknowledgments

The work has been supported through the Clinical Research Priority Program of the University of Zurich (CRPP Pain). N. Frezel has been supported through a Contrat Doctoral Specifique pour Normaliens (CDSN) grant awarded for a joint PhD at the University of Zürich and the Institute of Biology of the École Normale Supérieure (IBENS), Paris Sciences et Lettres Research University (PSL), Paris 75005, France. E. Platonova has been supported through the Technology Platform commission of the University of Zürich. We want to thank C. Kaiser for the technical support and F. Voigt and F. Helmchen for the support with the MesoSPIM.

Corresponding authors: zeilhofer@pharma.uzh.ch; hwildner@pharma.uzh.ch

Conflict of interest.

No conflict of interest.

Abbreviations

CST: corticospinal tract; rAAV: recombinant adeno-associated virus; RVM: rostral ventromedial medulla; S1: primary somatosensory cortex; S1hl: hindlimb area of S1; S1-CST: corticospinal tract originating in S1; 7N: facial nuclei, ACC: anterior cingulate cortex, MnR: median raphe nucleus, PAG: Periaqueductal grey, S1hl: somatosensory cortex, hindlimb area.VPL: ventral posterolateral nucleus of the thalamus; WGA: wheat germ agglutinin.

References

Abraira VE, Ginty DD. 2013. The sensory neurons of touch. Neuron. 79:618-639.

Abraira VE, Kuehn ED, Chirila AM, Springel MW, Toliver AA, Zimmerman AL, Orefice LL, Boyle KA, Bai L, Song BJ, Bashista KA, O'Neill TG, Zhuo J, Tsan C, Hoynoski J, Rutlin M, Kus L, Niederkofler V, Watanabe M, Dymecki SM, Nelson SB, Heintz N, Hughes DI, Ginty DD. 2017. The cellular and synaptic architecture of the mechanosensory dorsal horn. Cell. 168:295-310 e219.

Albisetti GW, Ghanem A, Foster E, Conzelmann KK, Zeilhofer HU, Wildner H. 2017. Identification of two classes of somatosensory neurons that display resistance to retrograde infection by rabies virus. J Neurosci. 37:10358-10371.

Albisetti GW, Pagani M, Platonova E, Hosli L, Johannssen HC, Fritschy JM, Wildner H, Zeilhofer HU. 2019. Dorsal horn gastrin-releasing peptide expressing neurons transmit spinal itch but not pain signals. J Neurosci. 39:2238-2250.

Arlotta P, Molyneaux BJ, Chen J, Inoue J, Kominami R, Macklis JD. 2005. Neuronal subtype-specific genes that control corticospinal motor neuron development in vivo. Neuron. 45:207-221.

Bareyre FM, Kerschensteiner M, Misgeld T, Sanes JR. 2005. Transgenic labeling of the corticospinal tract for monitoring axonal responses to spinal cord injury. Nat Med. 11:1355-1360.

Bourane S, Grossmann KS, Britz O, Dalet A, Del Barrio MG, Stam FJ, Garcia-Campmany L, Koch S, Goulding M. 2015. Identification of a spinal circuit for light touch and fine motor control. Cell. 160:503-515.

Callaway EM, Luo L. 2015. Monosynaptic circuit tracing with glycoprotein-deleted rabies viruses. J Neurosci. 35:8979-8985.

Casale EJ, Light AR, Rustioni A. 1988. Direct projection of the corticospinal tract to the superficial laminae of the spinal cord in the rat. The Journal of comparative neurology. 278:275-286.

Cheng L, Duan B, Huang T, Zhang Y, Chen Y, Britz O, Garcia-Campmany L, Ren X, Vong L, Lowell BB, Goulding M, Wang Y, Ma Q. 2017. Identification of spinal circuits involved in touch-evoked dynamic mechanical pain. Nature neuroscience. 20:804-814.

Ciabatti E, Gonzalez-Rueda A, Mariotti L, Morgese F, Tripodi M. 2017. Life-long genetic and functional access to neural circuits using self-inactivating rabies virus. Cell. 170:382-392 e314.

Constantinople CM, Bruno RM. 2013. Deep cortical layers are activated directly by thalamus. Science. 340:1591-1594.

Del Barrio MG, Bourane S, Grossmann K, Schule R, Britsch S, O'Leary DD, Goulding M. 2013. A transcription factor code defines nine sensory interneuron subtypes in the mechanosensory area of the spinal cord. PLoS One. 8:e77928.

Foster E, Wildner H, Tudeau L, Haueter S, Ralvenius WT, Jegen M, Johannssen H, Hosli L, Haenraets K, Ghanem A, Conzelmann KK, Bosl M, Zeilhofer HU. 2015. Targeted ablation, silencing,

and activation establish glycinergic dorsal horn neurons as key components of a spinal gate for pain and itch. Neuron. 85:1289-1304.
Fry EJ, Chagnon MJ, Lopez-Vales R, Tremblay ML, David S. 2010. Corticospinal tract regeneration after spinal cord injury in receptor protein tyrosine phosphatase sigma deficient mice. Glia. 58:423-433.
Gilbert CD, Wiesel TN. 1979. Morphology and intracortical projections of functionally characterised neurones in the cat visual cortex. Nature. 280:120-125.
Haenraets K, Foster E, Johannssen H, Kandra V, Frezel N, Steffen T, Jaramillo V, Paterna JC, Zeilhofer HU, Wildner H. 2017. Spinal nociceptive circuit analysis with recombinant adeno-associated viruses: the impact of serotypes and promoters. Journal of neurochemistry. 142:721-733.
Haring M, Zeisel A, Hochgerner H, Rinwa P, Jakobsson JET, Lonnerberg P, La Manno G, Sharma N, Borgius L, Kiehn O, Lagerstrom MC, Linnarsson S, Ernfors P. 2018. Neuronal atlas of the dorsal horn defines its architecture and links sensory input to transcriptional cell types. Nature neuroscience. 21:869-880.
Harris KD, Shepherd GM. 2015. The neocortical circuit: themes and variations. Nature neuroscience. 18:170-181.
Hu J, Huang T, Li T, Guo Z, Cheng L. 2012. c-Maf is required for the development of dorsal horn laminae III/IV neurons and mechanoreceptive DRG axon projections. J Neurosci. 32:5362-5373.
Hutson TH, Verhaagen J, Yanez-Munoz RJ, Moon LD. 2012. Corticospinal tract transduction: a comparison of seven adeno-associated viral vector serotypes and a non-integrating lentiviral vector. Gene Ther. 19:49-60.
Jin D, Liu YY, Sun F, Wang XH, Liu XF, He ZG. 2015. Restoration of skilled locomotion by sprouting corticospinal axons induced by co-deletion of PTEN and SOCS3. Nat Commun. 6.
Jursky F, Nelson N. 1995. Localization of glycine neurotransmitter transporter (GLYT2) reveals correlation with the distribution of glycine receptor. Journal of neurochemistry. 64:1026-1033.
Kamiyama T, Kameda H, Murabe N, Fukuda S, Yoshioka N, Mizukami H, Ozawa K, Sakurai M. 2015. Corticospinal tract development and spinal cord innervation differ between cervical and lumbar targets. J Neurosci. 35:1181-1191.
Klingler E, De la Rossa A, Fievre S, Devaraju K, Abe P, Jabaudon D. 2019. A translaminar genetic logic for the circuit identity of intracortically projecting neurons. Curr Biol. 29:332-339 e335.
Lemon RN, Griffiths J. 2005. Comparing the function of the corticospinal system in different species: organizational differences for motor specialization? Muscle Nerve. 32:261-279.
Liu Y, Latremoliere A, Li X, Zhang Z, Chen M, Wang X, Fang C, Zhu J, Alexandre C, Gao Z, Chen B, Ding X, Zhou JY, Zhang Y, Chen C, Wang KH, Woolf CJ, He Z. 2018. Touch and tactile neuropathic pain sensitivity are set by corticospinal projections. Nature. 561:547-550.

Malmberg AB, Chen C, Tonegawa S, Basbaum AI. 1997. Preserved acute pain and reduced neuropathic pain in mice lacking PKCgamma. Science. 278:279-283.

Molyneaux BJ, Arlotta P, Menezes JRL, Macklis JD. 2007. Neuronal subtype specification in the cerebral cortex. Nat Rev Neurosci. 8:427-437.

Muller T, Brohmann H, Pierani A, Heppenstall PA, Lewin GR, Jessell TM, Birchmeier C. 2002. The homeodomain factor lbx1 distinguishes two major programs of neuronal differentiation in the dorsal spinal cord. Neuron. 34:551-562.

Peirs C, Williams SP, Zhao X, Walsh CE, Gedeon JY, Cagle NE, Goldring AC, Hioki H, Liu Z, Marell PS, Seal RP. 2015. Dorsal horn circuits for persistent mechanical pain. Neuron. 87:797-812.

Polgar E, Fowler JH, McGill MM, Todd AJ. 1999. The types of neuron which contain protein kinase C gamma in rat spinal cord. Brain Res. 833:71-80.

Porrero C, Rubio-Garrido P, Avendano C, Clasca F. 2010. Mapping of fluorescent protein-expressing neurons and axon pathways in adult and developing Thy1-eYFP-H transgenic mice. Brain Res. 1345:59-72.

Poyatos I, Ponce J, Aragon C, Gimenez C, Zafra F. 1997. The glycine transporter GLYT2 is a reliable marker for glycine-immunoreactive neurons. Mol Brain Res. 49:63-70.

Quiquempoix M, Fayad SL, Boutourlinsky K, Leresche N, Lambert RC, Bessaih T. 2018. Layer 2/3 pyramidal neurons control the gain of cortical output. Cell reports. 24:2799-2807 e2794.

Spike RC, Watt C, Zafra F, Todd AJ. 1997. An ultrastructural study of the glycine transporter GLYT2 and its association with glycine in the superficial laminae of the rat spinal dorsal horn. Neuroscience. 77:543-551.

Steward O, Zheng B, Tessier-Lavigne M, Hofstadter M, Sharp K, Yee KM. 2008. Regenerative growth of corticospinal tract axons via the ventral column after spinal cord injury in mice. J Neurosci. 28:6836-6847.

Taniguchi H, He M, Wu P, Kim S, Paik R, Sugino K, Kvitsiani D, Fu Y, Lu J, Lin Y, Miyoshi G, Shima Y, Fishell G, Nelson SB, Huang ZJ. 2011. A resource of Cre driver lines for genetic targeting of GABAergic neurons in cerebral cortex. Neuron. 71:995-1013.

Tervo DG, Hwang BY, Viswanathan S, Gaj T, Lavzin M, Ritola KD, Lindo S, Michael S, Kuleshova E, Ojala D, Huang CC, Gerfen CR, Schiller J, Dudman JT, Hantman AW, Looger LL, Schaffer DV, Karpova AY. 2016. A designer aav variant permits efficient retrograde access to projection neurons. Neuron. 92:372-382.

Tlamsa AP, Brumberg JC. 2010. Organization and morphology of thalamocortical neurons of mouse ventral lateral thalamus. Somatosens Mot Res. 27:34-43.

McMahon T, Koltzenburg M, Tracey I, Turk D. 2013. Ascending projection systems, Wall & Melzack's Textbook of Pain.

Ueno M, Nakamura Y, Li J, Gu Z, Niehaus J, Maezawa M, Crone SA, Goulding M, Baccei ML, Yoshida Y. 2018. Corticospinal circuits from the sensory and motor cortices differentially regulate skilled movements through distinct spinal interneurons. Cell reports. 23:1286-1300 e1287.

Voigt F, Kirschenbaum D, Platonova E, Pagès S, Campbell RAA, Kästli, Schaettin M, Egolf L, van der Bourg A, Bethge P, Haenraets K, Frézel N, Topilko T, Perin P, Hillier D, Hildebrand S, Schueth A, Roebroeck A, Roska B, Stoeckli E, Pizzala R, Renier N, Zeilhofer HU, Karayannis T, Ziegler U, Batti L, Holtmaat A, Lüscher C, Aguzzi A, Helmchen F. 2019. The mesoSPIM initiative: open-source light-sheet microscopes for imaging cleared tissue. Nature Methods.

Wang X, Liu Y, Li X, Zhang Z, Yang H, Zhang Y, Williams PR, Alwahab NSA, Kapur K, Yu B, Chen M, Ding H, Gerfen CR, Wang KH, He Z. 2017. Deconstruction of corticospinal circuits for goal-directed motor skills. Cell. 171:440-455 e414.

Wang Z, Maunze B, Wang Y, Tsoulfas P, Blackmore MG. 2018. Global connectivity and function of descending spinal input revealed by 3d microscopy and retrograde transduction. J Neurosci. 38:10566-10581.

Watakabe A, Ichinohe N, Ohsawa S, Hashikawa T, Komatsu Y, Rockland KS, Yamamori T. 2007. Comparative analysis of layer-specific genes in mammalian neocortex. Cerebral Cortex. 17:1918-1933.

Willenberg R, Steward O. 2015. Nonspecific labeling limits the utility of cre-lox bred cst-yfp mice for studies of corticospinal tract regeneration. Journal of Comparative Neurology. 523:2665-2682.

Xu X, Roby KD, Callaway EM. 2010. Immunochemical characterization of inhibitory mouse cortical neurons: three chemically distinct classes of inhibitory cells. The Journal of comparative neurology. 518:389-404.

Zeilhofer HU, Studler B, Arabadzisz D, Schweizer C, Ahmadi S, Layh B, Bosl MR, Fritschy JM. 2005. Glycinergic neurons expressing enhanced green fluorescent protein in bacterial artificial chromosome transgenic mice. The Journal of comparative neurology. 482:123-141.

Zeisel A, Munoz-Manchado AB, Codeluppi S, Lonnerberg P, La Manno G, Jureus A, Marques S, Munguba H, He L, Betsholtz C, Rolny C, Castelo-Branco G, Hjerling-Leffler J, Linnarsson S. 2015. Brain structure. Cell types in the mouse cortex and hippocampus revealed by single-cell RNA-seq. Science. 347:1138-1142.